

# Exploiting Defenses against GAN-Based Feature Inference Attacks in Federated Learning

**Xianglong Zhang**

*University of Science and Technology Beijing*

XLZHANG@XS.USTB.EDU.CN

**Xinjian Luo**

*National University of Singapore*

XINJLUO@COMP.NUS.EDU.SG

## Abstract

As a decentralized model training method, federated learning is designed to integrate the isolated data islands and protect data privacy. Recent studies, however, have demonstrated that the Generative Adversarial Network (GAN) based attacks can be used in federated learning to learn the distribution of the victim’s private dataset and accordingly reconstruct human-distinguishable images. In this paper, we exploit defenses against GAN-based attacks in federated learning, and propose a framework, Anti-GAN, to prevent attackers from learning the real distribution of the victim’s data. The core idea of Anti-GAN is to corrupt the visual features of the victim’s private training images, such that the images restored by the attacker are indistinguishable to human eyes. Specifically, in Anti-GAN, the victim first projects the personal dataset onto a GAN’s generator, then mixes the fake images generated by the generator with the real images to obtain the training dataset, which will be fed into the federated model for training. We redesign the structure of the victim’s GAN to encourage it to learn the classification features (instead of the visual features) of the real images. We further introduce an unsupervised task to the GAN model for obfuscating the visual features of the generated images. The experiments demonstrate that Anti-GAN can effectively prevent the attacker from learning the distribution of the private images, meanwhile causing little harm to the accuracy of the federated model.

**Keywords:** Federated Learning; Security; Privacy; GAN; Defense.

## 1. Introduction

Nowadays, Machine Learning (ML), especially deep learning, is playing a critical role in real-life applications, ranging from face recognition to robotics. Despite the popularity and impressive performance, ML algorithms are vulnerable to various attacks, such as model inversion (Fredrikson et al. (2015)), membership inference (Shokri et al. (2017); Salem et al. (2018)) and model extraction (Tramèr et al. (2016)). To protect the user-level privacy, as well as alleviate the problem of data fragmentation and isolation, McMahan et al. (2016) propose a distributed machine learning framework called *federated learning* (FL), which is performed among one server and multiple clients. The training process of FL iteratively proceeds in multiple rounds of communication to enable the clients to collaboratively train a shared model. Recent studies, however, have shown that feature inference attacks (Melis et al. (2019); Hitaj et al. (2017); Wang et al. (2019); Luo et al. (2020)) can be effectively applied to federated learning, causing unintended information leakage and model poisoning.

Generative Adversarial Network (GAN) is proposed by Goodfellow et al. (2014) to learn the distribution of training datasets. Given the impressive performance of GAN on data reconstruction, Hitaj et al. (2017) propose a GAN-based attack on federated learning, where an adversarial client locally trains a GAN model to deliberately learn the distribution of the victim’s private dataset based on the shared model gradients, then accordingly reconstruct the private images (e.g., face pictures). Wang et al. (2019) further exploit user-level privacy leakage by training a multi-task GAN model in a malicious central server. Hitaj et al. (2017) claim that it is difficult to defense such attacks as long as the classification accuracy of the victim’s local model is high enough. In this paper, we exploit defenses against GAN-based feature inference attacks in federated learning. For simplicity, we focus on deep neural networks, which is consistent with Hitaj et al. (2017) and Wang et al. (2019).

There are two main challenges to design defenses against GAN-based attacks in federated learning: the *first* is that the traditional cryptographic methods (e.g., homomorphic encryption and secure multiparty computation) consume considerable computational time and power, thus barely useful for edge devices (e.g., mobiles and wearable devices) in federated learning; the *second* is that adding noise to the shared gradients (e.g., differential privacy) can harm the convergence and performance of the federated model. Besides, Hitaj et al. (2017) have experimentally proved that differential privacy can hardly prevent the attacker from learning data distribution of the private dataset. To address these challenges, we propose a defense mechanism, Anti-GAN, to protect the victim’s private dataset from the GAN-based inference attacks. The core idea of Anti-GAN is to generate the training images via a GAN model, where the visual features of the generated images are obfuscated by a specifically designed loss function, such that the attacker’s GAN model can only learn the distribution of these visually indistinguishable images.

Considering that the distribution of the obfuscated images could be different from that of the real images, this strategy could degrade the accuracy (tested on the real images) of the federated model trained on the obfuscated images. To solve this problem, we redesign the structure of the victim’s GAN model such that the classification features, instead of the visual features, of the real images, will be learned. To further improve the performance of the federated model, we use a modified Mixup scheme (Zhang et al. (2017)) to generate the final training images by mixing the generated fake images with the real images. Specifically, the victim first trains a GAN model based on the private dataset  $X$ , then accordingly generates the fake images  $X'$ , such that  $X'$  and  $X$  have similar classification features while the visual features of  $X'$  are obfuscated. The generated  $X'$  is then mixed with  $X$  to obtain the training dataset  $\hat{X}$ , and  $\hat{X}$  is finally used to train the federated model. The framework of Anti-GAN is shown in Fig. 1. We conduct extensive experiments on MNIST (Yann et al. (1998)), CIFAR-10 and CIFAR-100 (Krizhevsky et al. (2009)) to evaluate the validity of Anti-GAN. The results demonstrate that Anti-GAN can effectively reduce the plausibility of the images reconstructed by the attacker’s GAN model, meanwhile causing little harm to the accuracy of the global federated model.

Our contributions are summarized as follows:

- We explore the defenses against GAN-based feature inference attacks in federated learning. The proposed defense framework, Anti-GAN, can effectively prevent the attacker from learning the distinguishable visual features of the victim’s private images.

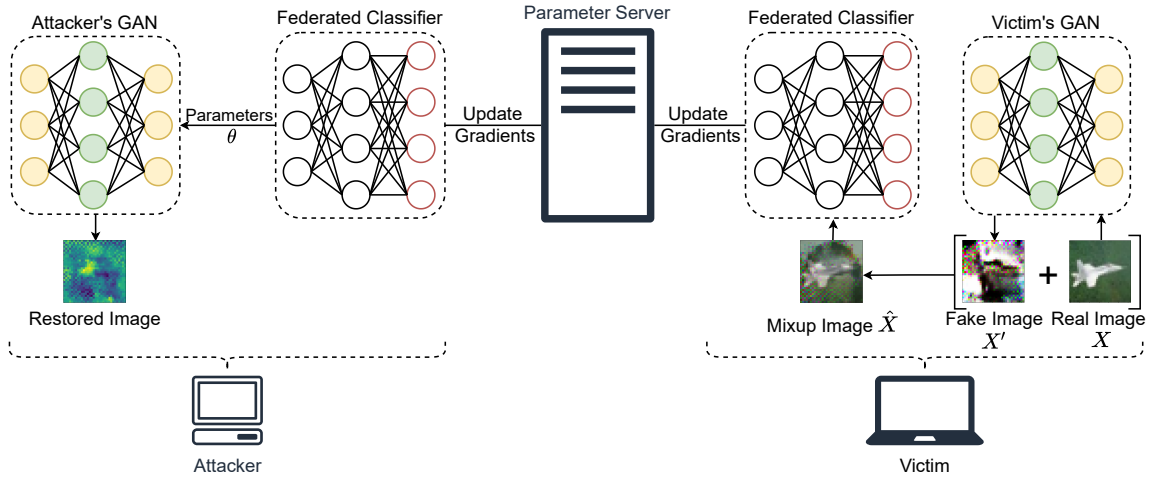


Figure 1: The defense framework of Anti-GAN.

- We introduce an unsupervised learning task to the victim’s GAN model for obfuscating the visual features of the generated images. We redesign the structure of the GAN model to maximally preserve the classification features of the real images.
- We conduct extensive experiments on three real-world datasets to evaluate the performance of Anti-GAN . The results demonstrate that our scheme can effectively protect private images from GAN-based inference attacks.

The rest of this paper is organized as follows. Section 2 gives the related work and background knowledge. The proposed defense framework is introduced in Section 3. The security of Anti-GAN and experimental results are discussed in Section 4 and 5, respectively. We summarize our work in Section 6.

## 2. Related Work and Background

In this paper, we propose a mechanism, called Anti-GAN, to defense against GAN-based attacks in federated learning. Before detailing Anti-GAN, we first introduce the related work and background, including federated learning, generative adversarial network and mainstream attacks to machine learning.

### 2.1. Federated Learning

A machine learning algorithm is a function mapping  $f_{\theta} : \mathcal{X} \mapsto \mathcal{Y}$  with respect to a set of parameters  $\theta$ , where  $\mathcal{X}$  is the input and  $\mathcal{Y}$  is the output. For image classification tasks,  $\mathcal{X}$  denotes a collection of images, and  $\mathcal{Y}$  denotes a set of labels corresponding to these images.

Federated learning (FL) is proposed by McMahan et al. (2016) to solve the data isolation problem and protect data privacy. The motivation of this concept is closely related to the rising of edge devices, e.g., mobiles, wearable devices. FL enables multiple data holders to collaboratively train a shared global model. The training process of FL proceeds in multiple rounds of communications: first, all clients agree on a specific structure of the global model;

then the server randomly selects a fraction of clients and sends the global model state to each client; finally, each selected client trains the model on their local data and exchange model gradients to each other via the server. Suppose  $N$  data holders  $\{\mathcal{F}_1, \dots, \mathcal{F}_N\}$  wish to train a shared model  $\mathcal{M}_{FED}$  with their respective data  $\{\mathcal{D}_1, \dots, \mathcal{D}_N\}$ . The objective of federated learning is:

$$\min_{\theta \in \mathbb{R}^d} L(\theta) \quad \text{where} \quad L(\theta) = \sum_{k=1}^N \frac{n_k}{n} \ell_k(\theta), \quad (1)$$

where  $n_k = |\mathcal{D}_k|$ , and  $n = \sum_{k=1}^N n_k$  is the total number of training points, and  $\ell_k(\theta) = \frac{1}{n_k} \sum_{i \in \mathcal{D}_k} \ell(x_i, y_i; \theta)$  is the loss of  $\mathcal{F}_k$ 's local model.  $\ell(x_i, y_i; \theta)$  denotes the loss of prediction on sample point  $(x_i, y_i)$  with parameters  $\theta$ .

## 2.2. Generative Adversarial Network (GAN)

Generative Adversarial Networks (GAN) is proposed by [Goodfellow et al. \(2014\)](#), then improved by [Radford et al. \(2015\)](#) as the Deep Convolutional Generative Adversarial Network (DCGAN), which is also the basis of most image-related studies.

A GAN model consists of a generator  $G$  and a discriminator  $D$ . The objective of  $G$  is to generate pseudo-samples  $G(z)$  from the random noise  $z$  such that  $G(z)$  is indistinguishable from the real sample  $x$  fed to  $D$ . The training process of GAN is like a facial composite imaging for police, where an artist ( $G$ ) generates a picture based on an eyewitness ( $D$ ) description of the suspect's face ([Hitaj et al. \(2017\)](#)). Typically,  $D$  and  $G$  play a minimax two-player game such that

$$\min_G \max_D V(D, G) = \mathbb{E}_{x \sim p_{data}(x)} [\log D(x)] + \mathbb{E}_{z \sim p_z(z)} [\log(1 - D(G(z)))], \quad (2)$$

where  $p_{data}$  denotes the original data distribution fed to discriminator  $D$ , and  $p_z$  denotes the prior distribution of noise variable  $z$ .  $D(x)$  is the probability output by  $D$  that  $x$  comes from the original training data rather than the generator.

However, the traditional GANs, including DCGAN and WGAN ([Arjovsky et al. \(2017\)](#)), can not label the generated images, thus having little benefits to the supervised image classification tasks. Instead, we use Conditional GAN (CGAN for short, [Mirza and Osindero \(2014\)](#)) to generate images and labels simultaneously. By feeding the labels  $y$  into both the generator and discriminator, CGAN can control the classes of the generated images:

$$\min_G \max_D V_C(D, G) = \mathbb{E}_{x \sim p_{data}(x)} [\log D(x|y)] + \mathbb{E}_{z \sim p_z(z)} [\log(1 - D(G(z|y)))]. \quad (3)$$

## 2.3. Attacks and Defenses in Machine Learning

Machine learning algorithms are vulnerable to various attacks, such as membership inference ([Shokri et al. \(2017\)](#); [Salem et al. \(2018\)](#); [Nasr et al. \(2019\)](#)), feature inference ([Fredrikson et al. \(2015\)](#)) and model extraction ([Tramèr et al. \(2016\)](#)). In this paper, we focus on the *feature inference* (or model inversion) attacks.

Feature inference attacks aim to restore the feature values from the private training datasets. [Fredrikson et al. \(2015\)](#) explore model inversion attacks in decision trees and

neural networks based on labels and black-box access to the target model. Luo et al. (2020) propose to infer the training data in federated learning by model predictions. Zhu and Han (2020) and Zhao et al. (2020) restore the private training data by only the model gradients. In federated learning, some newest studies exploit feature inference attacks based on GANs. Hitaj et al. (2017) propose a GAN-based threat model, in which an adversary tries to extract the training information of a class that is not owned by her. By taking the global model as the discriminator of GAN, the adversary can further mislabel the pseudo-samples generated by the generator so as to trick other participants to leak more private information. Wang et al. (2019) assume the server is malicious and utilize GAN to explore user-level privacy leakage, which is similar to Hitaj et al. (2017)’s work.

Several defenses have been proposed to alleviate the risks of data leakage, such as InstaHide (Huang et al. (2020)), anomaly detection (Bagdasaryan et al. (2018)), dropout (Melis et al. (2019); Salem et al. (2018)), differential privacy (Shokri and Shmatikov (2015); Bagdasaryan et al. (2018)), secure multiparty computation (Bonawitz et al. (2017)) and model stacking (Salem et al. (2018)), among which InstaHide is most similar to our scheme, i.e., using *Mixup* (Zhang et al. (2017)) to corrupt the visual features of private training images. The difference is that InstaHide mixes multiple real images into one training image, while we first use a GAN model to generate multiple fake images and then mix fake images with real images. In addition, Carlini et al. (2020) and Luo et al. (2021) have experimentally proved that InstaHide can hardly protect private images, whereas our scheme can provide better privacy protection compared to InstaHide. Besides, few methods have been proposed to defense the attacks in Hitaj et al. (2017) and Wang et al. (2019). To our best knowledge, this is also the first paper to exploit defenses against GAN-based feature inference attacks.

### 3. Approach

The proposed scheme, Anti-GAN, is used to defense GAN-based feature inference attacks in federated learning (Hitaj et al. (2017); Wang et al. (2019)). In this section, we first introduce the threat model of GAN-based attacks, then detail the framework of Anti-GAN.

#### 3.1. Threat Model

There are generally two types of threat models in GAN-based attacks: one or multiple participants are adversaries, e.g., Hitaj et al. (2017); the central server is the adversary, e.g., Wang et al. (2019). Nevertheless, the basic ideas under these attacks are similar, i.e., the attacker takes the global shared model as a discriminator, then trains a generator to reconstruct the victim’s private training images. For simplicity, we focus on the attack model in Hitaj et al. (2017).

In federated learning, all participants agree on a common global model before training. Suppose the central server is authoritative and can not be compromised by any adversaries. One participant  $A$ , acting as an adversary, owns data with labels  $[b, c]$ , and the victim  $V$  owns data with labels  $[a, b]$ . The objective of  $A$  is to reconstruct the data with label  $a$  owned by  $V$ . The *attacking process* is as follows: first,  $V$  honestly trains a local model and uploads the model gradients to the central server; second,  $A$  downloads these shared gradients and accordingly updates the discriminator of his GAN model. Then  $A$  generates a data point of label  $a$  from GAN and labels it as class  $c$ .  $A$  will train his local model

with these pseudo-samples and share the parameters to the global model to encourage  $V$  providing more information about  $a$  class. In the end,  $A$  can reconstruct an image of class  $a$  which is indistinguishable from  $V$ 's original images. Hitaj et al. (2017) claim that it is difficult to defense such attacks as long as the accuracy of the victim's local model is high enough.

### 3.2. The framework of Anti-GAN

We design a defense mechanism, Anti-GAN, to eliminate the data leakage risks incurred by GAN-based inference attacks. Note that the victim  $V$  is also called the *defender* in this paper since the defense method is performed by  $V$ . In Anti-GAN, we propose to obfuscate the visual features of training images fed into the federated classifier. The problem is how to incur little accuracy degradation when training the federated classifier on the obfuscated images.

In our scheme, to protect the private dataset  $X$ , the defender first trains a CGAN model based on  $X$ , then generates a shadow image set  $X'$  via this CGAN and mixes  $X'$  with  $X$  to generate the final training images  $\hat{X}$  (Fig. 1). We design new loss functions for the defender's GAN to guarantee that the classification feature maps of  $X'$  are similar to that of  $X$ , meanwhile the visual features of  $X'$  are hardly distinguishable to human, such that the images restored by the attack's GAN will demonstrate little plausible visual features.

#### 3.2.1. OBFUSCATING VISUAL FEATURES

Given that the defender uses the generated samples  $X'$  as the training data, the adversary could reconstruct a plausible image using his own GAN model by learning the distribution of  $X'$ , e.g., generating a plausible image to human. To reduce the risk of privacy leakage, we need to obfuscate the visual features of  $X'$  to prevent the adversary from generating distinguishable images.

Note that GAN tends to produce sharp images (Isola et al. (2017)). Inspired by PatchShuffle (Kang et al. (2017)), we find window-wise transformations to an image  $x$  can obfuscate the local visual features (e.g., edges and corners) while preserving the overall features (e.g., image patterns) of  $x$ . Therefore, we introduce an unsupervised learning task to the defender's generator  $G$  to obfuscate the window-wise visual features of the generated images. Specifically, for an image  $x'$  generated by  $G$ , we first split  $x'$  into  $n$  windows of size  $s \times s$ , then compute the following loss function:

$$\min_G \mathcal{L}_{\text{obf}} \quad \text{where} \quad \mathcal{L}_{\text{obf}} = \sum_i (Var(\mathbf{w}_i(G(z))) - v_e)^2, \quad (4)$$

where  $Var(\mathbf{w}_i)$  denotes the pixel variance of window  $\mathbf{w}_i$ ;  $v_e$  is the *expected variance*, controlling the obfuscation level for each window. To help illustrate the effects of  $\mathcal{L}_{\text{obf}}$ , we use the gradient descending method to change the pixel values of an image according to Eq. 4 with different  $v_e$ . The results are shown in Fig. 2a. By setting a variance threshold  $v_e$  closing to the real image variance (e.g., 0.5), the defender can preserve the features of patches containing salient structures, while introducing much noise to the flat patches, i.e., the background. By setting a larger  $v_e$  (e.g., 0.8), more noise is introduced to obfuscate the entire image but the overall features are still preserved.



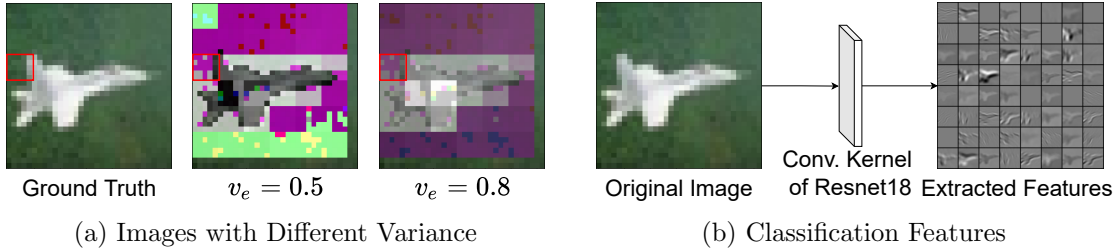


Figure 2: (a) some examples resulted from Eq. 4. The red box denotes a  $5 \times 5$  window. The image pixels are normalized into  $[-1, 1]$  beforehand; (b) the features extracted by the first convolutional layer of ResNet-18.

### 3.2.2. PRESERVING CLASSIFICATION FEATURES

GAN is used to learn the distribution of the training dataset  $X$  by an adversarial process (Goodfellow et al. (2014)). The loss function  $\mathcal{L}_{\text{obf}}$  in Eq. 4, however, can restrain the learning process of GAN, since  $\mathcal{L}_{\text{obf}}$  encourages the generator to produce images  $X'$  with pixel variance  $v_e$ , which could be different from the original variance of  $X$ . Considering that we use  $X'$  to train the federated model  $f$ , the test accuracy of  $f$  on the real images  $X$  could decrease since the distribution of the training dataset  $X'$  could be different from that of the testing dataset  $X$ . The problem is how to redesign the learning process of GAN such that the performance of the federated model trained on the generated images  $X'$  suffers little degradation.

In our setting, an image  $x'$  generated by GAN will be fed into the federated classifier, then this classifier determines the class of  $x'$  based on the classification features extracted by a series of convolutional and pooling layers. In other words, to reduce the performance degradation of the federated model after replacing the input  $X$  with  $X'$ , we only need to guarantee that the GAN correctly learns the distribution of the classification features of  $X$ , instead of the distribution of the visual features. Notice that the features extracted by a higher layer (e.g., the final dense layer) are more specific to the network structure, whereas the features extracted by a lower layer (e.g., the first convolutional layer) are more general in different tasks (Yosinski et al. (2014)). Given that the federated model will be trained only after the defender generates  $X'$ , we choose to use the first convolutional layer of the ResNet (He et al. (2016)) pre-trained on ImageNet (Deng et al. (2009)) as the *feature extractor* to extract the low-level image features, as shown in Fig. 2b. Since the feature extractor is pre-trained on ImageNet, it can extract extensive features and should be general enough for different classification tasks.

Based on this insight, we modify the objective function of CGAN as follows:

$$\min_G \max_D \mathcal{L}_{\text{CGAN}} = \mathbb{E}_{x \sim p_{\text{data}}(x)} [\log D(C(x)|y)] + \mathbb{E}_{z \sim p_z(z)} [\log(1 - D(C(G(z)|y)))], \quad (5)$$

where  $C(x)$  denotes the features of  $x$  extracted by the feature extractor  $C$ . In brief, instead of distinguishing  $x$  from  $x'$ , the task of the discriminator becomes distinguishing  $C(x)$  from  $C(x')$ . In summary, the final objective of the defender's GAN is

$$G^*(z^*) = \arg \min_G \max_D \mathcal{L}_{\text{CGAN}} + \min_G \lambda \mathcal{L}_{\text{obf}}, \quad (6)$$

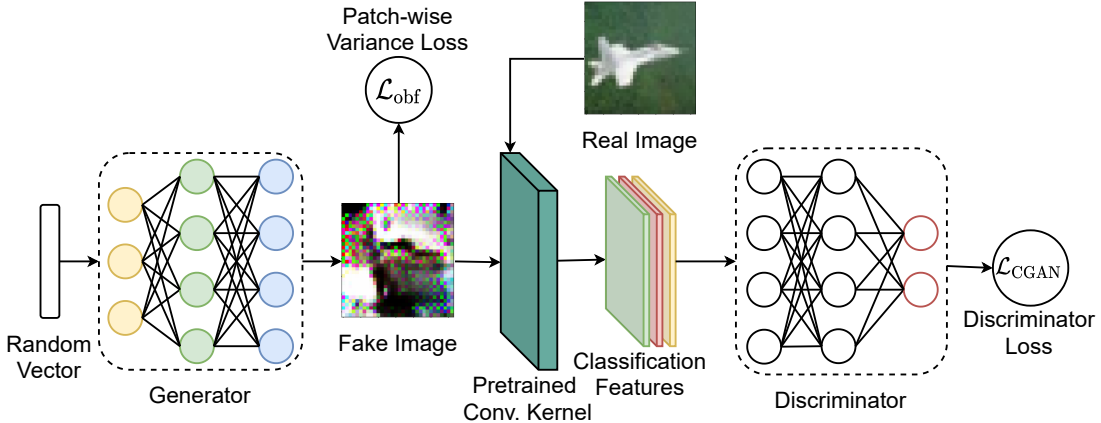


Figure 3: The structure of the defender’s GAN model.

where  $\lambda$  is a hyper parameter controlling the effect of  $\mathcal{L}_{obf}$ . The structure of the revised GAN model is shown in Fig. 3.

### 3.2.3. MIXUP

After training a CGAN model based on Eq. 6, the defender can generate  $X'$  and use it as the training images of the federated model. But in the experiments, we find the federated model trained on  $X'$  suffers an accuracy degradation (tested on  $X$ ) of roughly 20% compared to the model directly trained on  $X$ . The reason is that although the adopted feature extractor  $C$  is general, it is slightly different from the first convolutional layer of the trained federated model, thus the features learned by the GAN ( $\mathcal{L}_{CGAN}$ ) are less useful in the federated classification task. To further improve the performance of the federated model trained on  $X'$ , we use Mixup (Zhang et al. (2017)) to combine the distributions of  $X$  and  $X'$ .

As a data augmentation method, Mixup (Zhang et al. (2017)) is initially proposed to enhance the generalization of classification models. Specifically, Mixup generates a training image  $\hat{x}$  by mixing two randomly selected private images:  $\hat{x} = \mu x_1 + (1 - \mu)x_2$ , where  $\mu$  is a random number sampled from  $[0, 1]$ . The label  $\hat{y}$  is accordingly generated by  $\hat{y} = \mu y_1 + (1 - \mu)y_2$ , where  $y_1$  and  $y_2$  are one-hot labels. Considering that the one-hot label  $\hat{y}$  can leak the mixup parameter  $\mu$  (Huang et al. (2020); Luo et al. (2021)), we employ a revised scheme in Anti-GAN to enhance the security of Mixup: given a class  $c$ , we first randomly sample a real image  $x$  with label  $c$  from  $X$ , then generate an image  $x'$  with label  $c$  from the defender’s CGAN. The training image  $\hat{x}$  is generated by:

$$\hat{x} = \mu x + (1 - \mu)x', \tag{7}$$

where  $\mu$  is a tunable hyperparameter. The label  $\hat{y}$  of  $\hat{x}$  becomes  $c$  and leaks no information of  $\mu$ . To defend the current attacks on Mixup (Huang et al. (2020); Luo et al. (2021)), we mix each real image  $x$  only once, which means the training dataset  $\hat{X}$  contains only a portion of the information of  $X$ . The security analysis of this method is shown in Section 4.



## 4. Security Analysis

We now consider the security of Anti-GAN in federated learning.

**Attack scenario:** the defender generates the training dataset  $\hat{X}$  by mixing the real dataset  $X$  and the dataset  $X'$  produced by a CGAN model. In each epoch, the defender first feeds the  $(\hat{x}, \hat{y})$  pairs into the local federated model  $f$  to obtain the model gradients  $\nabla f$ , then uploads a percentage of gradients  $[\nabla f]$  to the parameter server (Hitaj et al. (2017)). The attacker downloads  $[\nabla f]$  from the server and infers the information of the private dataset  $X$  from  $[\nabla f]$ .

The security arguments consist of two halves: (1) to restore the information of  $X$ , the attacker has to recover the distribution of  $\hat{X}$ ; (2) restoring  $X$  from  $\hat{X}$  is difficult.

For the first argument, since the gradients  $[\nabla f]$  are computed based on the training images  $\hat{X}$ , an attacker with unlimited capacity can accurately recover the training images  $\hat{X}$ ; while a computationally limited attacker can only infer the distribution of  $\hat{X}$  via a GAN model. Nevertheless, both of these two attackers can not directly infer the information of  $X$  from  $[\nabla f]$  because  $\hat{X}$  is the only input for the computation of  $[\nabla f]$ . Note that the  $\hat{X}$  is generated by mixing  $X$  and  $X'$ . The visual features of  $X'$  are corrupted by  $\mathcal{L}_{\text{obf}}$  (Eq. 4), and the visual features of  $X$  are also corrupted by mixing with  $X'$ . The attackers with or without unlimited capacity can not infer the visual features of  $X$  from  $\hat{X}$ .

For the second argument, suppose the attacker has limited computational power, then this attacker can obtain the distribution of  $\hat{X}$ . As mentioned before, the visual features of  $\hat{X}$  are corrupted, thus the images restored by the attacker’s GAN model are indistinguishable to human eyes. Separating the distribution of  $X$  from  $\hat{X}$  is difficult since the attacker knows nothing about the mixing parameter  $\mu$  and the distribution of  $X'$ . Suppose the attacker has unlimited capacity, then this attacker can restore the original images of  $\hat{X}$ . We convert the attacker’s objective to the one that, given  $\hat{x}$ , restore the information of  $x$ . Although the  $\hat{x}$  is generated based on a linear transformation on  $x$  (Eq. 7), we mix each real image only once, which means that the  $x'$  acts as a one-time mask on the real image  $x$ . The attacker can not infer the information of  $x$  from  $\hat{x}$  as long as the mask  $x'$  is private. In addition, our mix-only-once strategy can defense the state-of-the-art attacks on Mixup (Carlini et al. (2020); Huang et al. (2020); Luo et al. (2021)) because these attacks only consider the scenario that one image is mixed multiple times.

## 5. Experiments

This section gives the experimental results on Anti-GAN. We first conduct an ablation study to verify the effectiveness of different components of Anti-GAN in Section 5.2, then analyze the impact of different expected variance  $v_e$  and Mixup parameter  $\mu$  on the model accuracy degradation and attacking results in Section 5.3 and 5.4, respectively.

### 5.1. Experimental Setting

**Datasets.** We use three image datasets MNIST (Yann et al. (1998)), CIFAR-10 and CIFAR-100 (Krizhevsky et al. (2009)) to evaluate the performance of Anti-GAN. The image size is  $32 \times 32$ . We normalize all the image pixels into  $[-1, 1]$  before the experiments.

**Metrics.** We focus on the accuracy degradation of the federated model caused by Anti-GAN, instead of the absolute model accuracy. In all the experiments, we use the original images  $X$  as the testing images, which is applicable to real-world applications. The accuracy *baseline* is the testing accuracy  $a_X$  of the model trained on real images  $X$ , i.e., the model accuracy trained by the original federated learning method. We first evaluate the testing accuracy  $a_{\hat{X}}$  of the model trained on  $\hat{X}$  generated by Anti-GAN, then compute the **A**ccuracy **D**egradation **R**atio (ADR) by  $\text{ADR} = (a_X - a_{\hat{X}})/a_X$ . Note that for ADR, lower is better.

**Implementation.** We use CGAN as the defender’s GAN model, where the first convolutional layer of the ResNet-18<sup>1</sup> pre-trained on ImageNet is adopted as the feature extractor. The attacker’s GAN model is DCGAN, which is consistent with Hitaj et al. (2017). All the neural networks are implemented in PyTorch<sup>2</sup> and trained with the Adam optimizer (Kingma and Ba (2014)) using an learning rate  $10^{-4}$ . All the experiments are performed on a platform with NVIDIA GTX2060 GPU and AMD R7 4800H CPU. For simplicity, we first empirically set the window size of  $\mathcal{L}_{\text{obf}}$  in Eq. 4 to  $5 \times 5$  and the coefficient  $\lambda$  of  $\mathcal{L}_{\text{obf}}$  in Eq. 6 to 1000 under MNIST and 100 under CIFAR, then focus on comparing the impact of different variance threshold  $v_e$  (Eq. 4) and mixup parameter  $\mu$  (Eq. 7) on the model accuracy degradation and attacking results. In the experiments, we find that a successful attack of Hitaj et al. (2017) needs careful model tuning and tricky timing, which is hardly achieved in the federated learning protected by Anti-GAN. Therefore, to better evaluate the performance of our scheme, we use a more powerful attack model, in which the attacker has direct black-box access to the defender’s dataset. That is, this attacker can use the defender’s private images to train a GAN model but not directly accessing them. In this setting, the attacker can learn a more accurate distribution of the defender’s data compared to learning the data distribution from the model gradients in Hitaj et al. (2017), causing more leakage risks to the defender’s data. For each dataset, we let the defender holds images with all classes. Then we attack the images of each class and compare the results.

## 5.2. Ablation Study












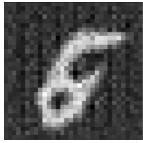


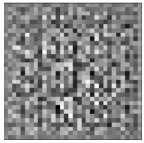
Anti-GAN consists of three main components: the loss function  $\mathcal{L}_{\text{obf}}$  for obfuscating the visual features of  $X'$ , the feature extractor for preserving the classification features of  $X$  in  $X'$ , and the Mixup step for improving the performance of the federated model. To validate the effectiveness of these components, we remove each component in turn and test the performance of the modified Anti-GAN on the MNIST dataset. Note that for the branches with Mixup, we set the parameter  $\mu = 0.5$ ; for the branches with  $\mathcal{L}_{\text{obf}}$ , we set the expected variance  $v_e = 0.4$  (Eq. 4). Tab. 1 shows the ADR of the trained federated models and some samples in  $X$ ,  $X'$  and  $\hat{X}$  under different branches of Anti-GAN, from which we have three main observations.

The first is that the model trained under the Anti-GAN without  $\mathcal{L}_{\text{obf}}$  achieves the least accuracy degradation, whereas the attacker can restore the private images with the best visual features, which means that this Anti-GAN can hardly protect the defender’s private images from GAN-based attacks. This is expected since, without  $\mathcal{L}_{\text{obf}}$ , the visual features

---

1. [https://pytorch.org/hub/pytorch\\_vision\\_resnet/](https://pytorch.org/hub/pytorch_vision_resnet/)  
 2. <https://pytorch.org/>

Table 1: Results of the ablation study.

Branch	The Original Anti-GAN	No $\mathcal{L}_{\text{obf}}$	No Feature Extractor	No Mixup
ADR	5%	4.1%	11%	22.4%
Example of $x$				
Example of $x'$				
Example of $\hat{x}$				/
Attack Result				

of  $X'$  learned by the defender’s GAN is roughly the same as the visual features of  $X$ , thus providing little protection for the private images  $X$ .

The second is that the model trained under the Anti-GAN without Mixup has the worst accuracy performance whereas the attacker can learn nothing from the training images  $X'$  generated by the defender’s GAN model. As mentioned in Section 3.2.3, the classification features learned by the modified GAN model could deviate from the classification features extracted by the federated model, leading to the case that the distribution of the training images  $X'$  is slightly different from that of the testing images  $X$ , which means the federated model performance will fairly degrade.

The third is that in the Anti-GAN without the feature extractor, the defender’s GAN model turns to learn the original distribution of  $X$  ( $\mathcal{L}_{\text{CGAN}}$ ), while the  $\mathcal{L}_{\text{obf}}$  encourages the GAN to learn a distorted distribution of  $X$ , i.e., a distribution with the expected variance  $v_e$ . As a result, the learned distribution is slightly different from the distribution of  $X$ . Although this Anti-GAN can protect the private images, it also causes considerable performance degradation to the federated model, which renders this design useless in real-world applications.

In summary, from Tab. 1, we observe that the original Anti-GAN can achieve the best trade-off between model performance degradation and privacy protection, validating the effectiveness of the proposed scheme.

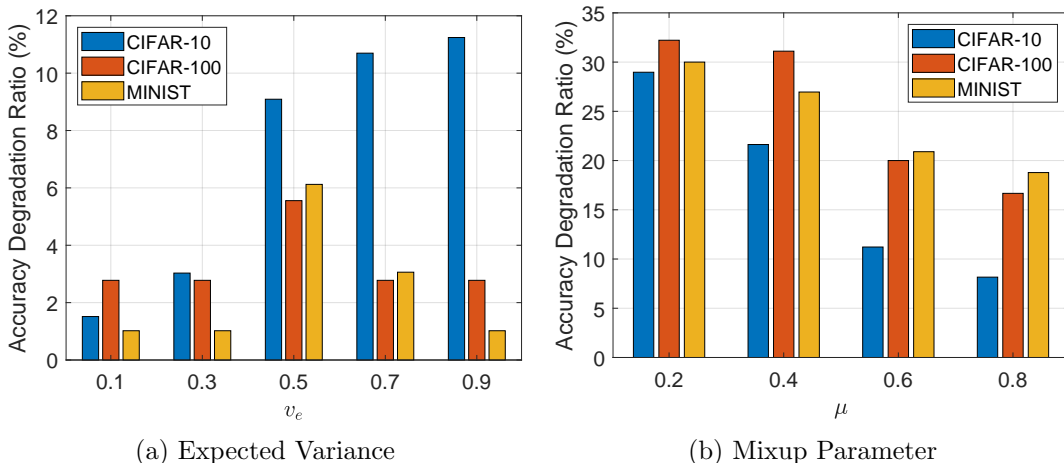


Figure 4: The ADR caused by (a) different expected variance  $v_e$  and (b) different Mixup parameter  $\mu$ .

### 5.3. Impact of Different Expected Variance $v_e$

$v_e$  is the expected variance in  $\mathcal{L}_{\text{obf}}$  (Eq. 4), controlling the level of visual feature obfuscation. In this section, we study the impact of different  $v_e$  on the model performance degradation and attack results, i.e., the distinguishability of the images restored by the attacker. The Mixup parameter  $\mu$  is fixed to 0.6.

To explore the model performance degradation caused by different  $v_e$ , we first train different federated models based on MNIST, CIFAR-10 and CIFAR-100 with different  $v_e$ , then compute the corresponding ADRs, which are shown in Fig. 4a. We show the images restored by the attacker under different  $v_e$  in Fig. 5.

From Fig. 4a, we observe that with the increase of  $v_e$ , the ADR of the models trained on CIFAR-10 increases, while the ADR of the models trained on CIFAR-100 and MNIST first rises then descends. The reason is that the object patterns of CIFAR-10 are more complex than the other two datasets, e.g., the background of the car images in CIFAR-10 varies greatly. As a result, a bigger  $v_e$  can increase the difficulty of learning the distribution of CIFAR-10 for the defender’s GAN model, thus causing more performance degradation. For the MNIST and CIFAR-100 datasets with simpler patterns, when  $v_e$  is set close to the real variance (i.e., 0.5), the  $\mathcal{L}_{\text{obf}}$  will focus on obfuscating the features of flat patches, e.g., the background, while preserving more visual features of the patches with salients structures, e.g., corners and edges. In this way, the distribution of the classification features of the generated images could deviate from the real classification feature distributions, leading to performance degradation. When the  $v_e$  is set to a value far from the real variance, the  $\mathcal{L}_{\text{obf}}$  will obfuscate the visual features of all patches, thus the classification features of the entire image can be well preserved. Nevertheless, we see that different  $v_e$  cause little harm ( $< 5\%$ ) to the model performance trained on MNIST and CIFAR-100.

From Fig. 5, we observe that under different  $v_e$ , the attacker can restore some distinguishable images from the MNIST dataset, while restoring little visual features from the CIFAR-10 dataset. The reason is that the MNIST dataset has only one channel and simple object patterns, making it easily learned and restored by the attacker’s GAN model. While

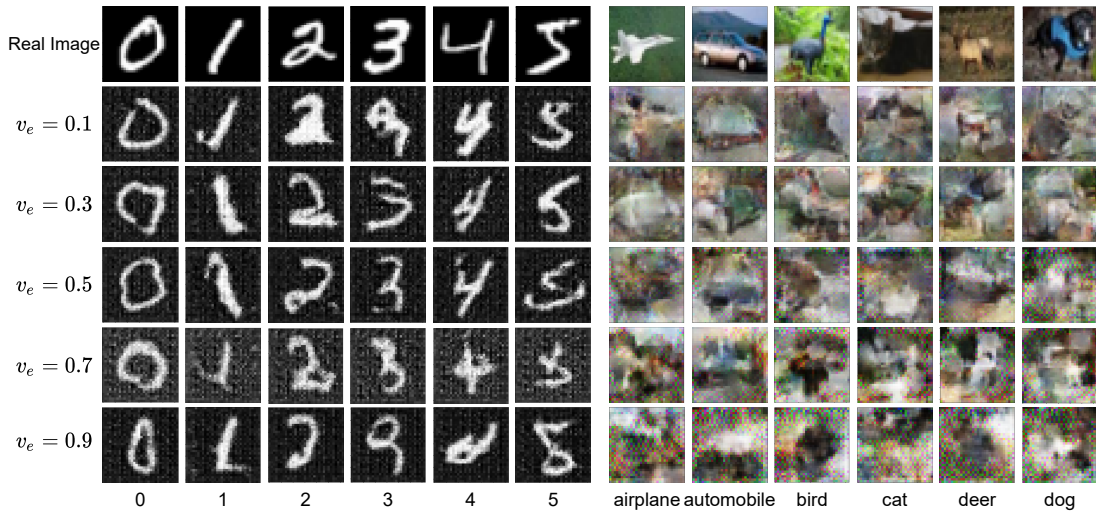


Figure 5: The images restored by the attacker under different expected variance  $v_e$ . The left part shows the MNIST images, and the right part shows the CIFAR-10 images.

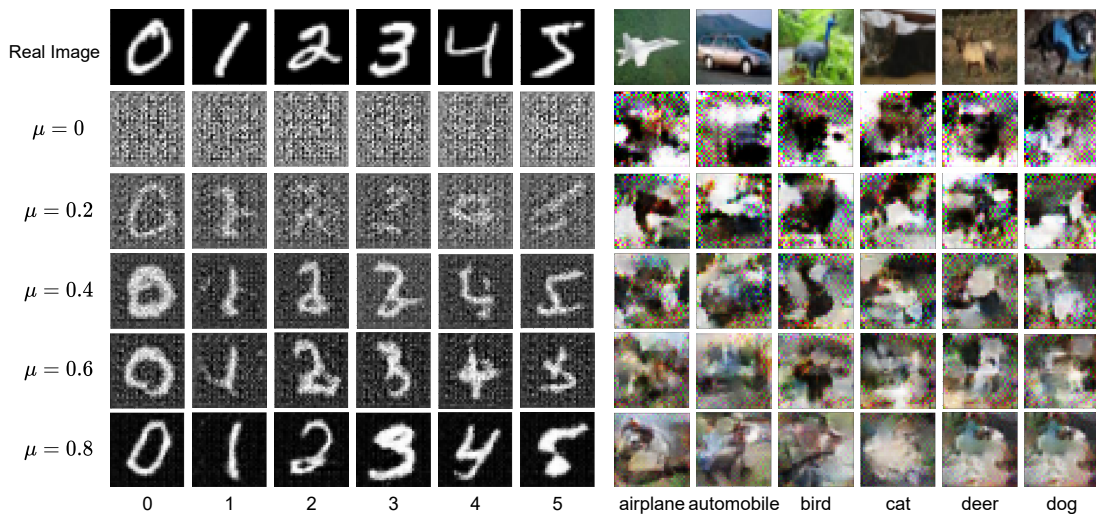


Figure 6: The images restored by the attacker under different Mixup parameter  $\mu$ . The left part shows the MNIST images, and the right part shows the CIFAR-10 images.

the CIFAR-10 dataset has three channels with more complex image patterns, bringing more difficulty in learning the distribution of the training images.

#### 5.4. Impact of Different Mixup Parameters $\mu$

In this section, we study the impact of different mixup parameters  $\mu$  on the model performance and attack results. The expected variance  $v_e$  is fixed to 0.7. The Mixup parameter  $\mu$  controls how much information of the real images  $X$  is contained in the training



images  $\hat{X}$  (Eq. 7). We test the ADR of federated models trained under different  $\mu$  based on MNIST, CIFAR-10 and CIFAR-100, and report the results in Fig. 4b.

We observe that with the increase of  $\mu$ , the federated models achieve less accuracy degradation, i.e., better performance. The reason is that with the increase of  $\mu$ , the portion of the real images  $X$  in the training images  $\hat{X}$  is accordingly increased, which means the distribution of the training images  $\hat{X}$  is closer to the distribution of the real images  $X$ , leading to less performance degradation compared to the original training method (both the training and testing datasets are  $X$ ).

Fig. 6 demonstrate the images restored by the attacker under different  $\mu$ . We see that for the MNIST dataset with simple object patterns, the attacker can restore better images with the increasing of  $\mu$ . This is expected because a larger  $\mu$  means a larger portion of the real image  $x$  in the Mixup image  $\hat{x}$ , and the visual features of  $\hat{x}$  become closer to the visual features of  $x$ , causing more risks of information leakage. For the CIFAR-10 dataset with more complex patterns, we observe that the attacker can hardly restore images with distinguishable visual features under different  $\mu$ , which means that the proposed scheme can provide enough protection for the private images even though mixing some real images into the training dataset.

## 6. Conclusion

Federated learning is vulnerable to GAN-base feature inference attacks, which are difficult to defense as long as the victim’s local model has good performance. In this paper, we propose a defense framework, Anti-GAN, to protect the victim’s private data from GAN-based attacks. Anti-GAN can distort the original distribution of the private training data to prevent attackers from generating distinguishable images, meanwhile causing little harm to the performance of the federated classifier.

## References

- Martin Arjovsky, Soumith Chintala, and Léon Bottou. Wasserstein gan. *arXiv preprint arXiv:1701.07875*, 2017.
- Eugene Bagdasaryan, Andreas Veit, Yiqing Hua, Deborah Estrin, and Vitaly Shmatikov. How to backdoor federated learning. *arXiv preprint arXiv:1807.00459*, 2018.
- Keith Bonawitz, Vladimir Ivanov, Ben Kreuter, Antonio Marcedone, H Brendan McMahan, Sarvar Patel, Daniel Ramage, Aaron Segal, and Karn Seth. Practical secure aggregation for privacy-preserving machine learning. In *Proceedings of the 2017 ACM SIGSAC Conference on Computer and Communications Security*, pages 1175–1191, 2017.
- Nicholas Carlini, Samuel Deng, Sanjam Garg, Somesh Jha, Saeed Mahloujifar, Mohammad Mahmoody, Shuang Song, Abhradeep Thakurta, and Florian Tramèr. An attack on instahide: Is private learning possible with instance encoding? *arXiv preprint arXiv:2011.05315*, 2020.



- Jia Deng, Wei Dong, Richard Socher, Li-Jia Li, Kai Li, and Li Fei-Fei. Imagenet: A large-scale hierarchical image database. In *2009 IEEE conference on computer vision and pattern recognition*, pages 248–255. Ieee, 2009.
- Matt Fredrikson, Somesh Jha, and Thomas Ristenpart. Model inversion attacks that exploit confidence information and basic countermeasures. In *Proceedings of the 22nd ACM SIGSAC Conference on Computer and Communications Security*, pages 1322–1333, 2015.
- Ian Goodfellow, Jean Pouget-Abadie, Mehdi Mirza, Bing Xu, David Warde-Farley, Sherjil Ozair, Aaron Courville, and Yoshua Bengio. Generative adversarial nets. In *Advances in neural information processing systems*, pages 2672–2680, 2014.
- Kaiming He, Xiangyu Zhang, Shaoqing Ren, and Jian Sun. Deep residual learning for image recognition. In *Proceedings of the IEEE conference on computer vision and pattern recognition*, pages 770–778, 2016.
- Briland Hitaj, Giuseppe Ateniese, and Fernando Perez-Cruz. Deep models under the gan: information leakage from collaborative deep learning. In *Proceedings of the 2017 ACM SIGSAC Conference on Computer and Communications Security*, pages 603–618, 2017.
- Yangsibo Huang, Zhao Song, Kai Li, and Sanjeev Arora. Instahide: Instance-hiding schemes for private distributed learning. In *International Conference on Machine Learning*, pages 4507–4518. PMLR, 2020.
- Phillip Isola, Jun-Yan Zhu, Tinghui Zhou, and Alexei A Efros. Image-to-image translation with conditional adversarial networks. In *Proceedings of the IEEE conference on computer vision and pattern recognition*, pages 1125–1134, 2017.
- Guoliang Kang, Xuanyi Dong, Liang Zheng, and Yi Yang. Patchshuffle regularization. *arXiv preprint arXiv:1707.07103*, 2017.
- Diederik P Kingma and Jimmy Ba. Adam: A method for stochastic optimization. *arXiv preprint arXiv:1412.6980*, 2014.
- Alex Krizhevsky, Geoffrey Hinton, et al. Learning multiple layers of features from tiny images. 2009.
- Xinjian Luo, Yuncheng Wu, Xiaokui Xiao, and Beng Chin Ooi. Feature inference attack on model predictions in vertical federated learning. *arXiv preprint arXiv:2010.10152*, 2020.
- Xinjian Luo, Xiaokui Xiao, Yuncheng Wu, Juncheng Liu, and Beng Chin Ooi. A fusion-denoising attack on instahide with data augmentation. *arXiv preprint arXiv:2105.07754*, 2021.
- H Brendan McMahan, Eider Moore, Daniel Ramage, Seth Hampson, et al. Communication-efficient learning of deep networks from decentralized data. *arXiv preprint arXiv:1602.05629*, 2016.
- Luca Melis, Congzheng Song, Emiliano De Cristofaro, and Vitaly Shmatikov. Exploiting unintended feature leakage in collaborative learning. In *2019 IEEE Symposium on Security and Privacy (SP)*, pages 691–706. IEEE, 2019.

- Mehdi Mirza and Simon Osindero. Conditional generative adversarial nets. *arXiv preprint arXiv:1411.1784*, 2014.
- Milad Nasr, Reza Shokri, and Amir Houmansadr. Comprehensive privacy analysis of deep learning: Passive and active white-box inference attacks against centralized and federated learning. In *2019 IEEE symposium on security and privacy (SP)*, pages 739–753. IEEE, 2019.
- Alec Radford, Luke Metz, and Soumith Chintala. Unsupervised representation learning with deep convolutional generative adversarial networks. *arXiv preprint arXiv:1511.06434*, 2015.
- Ahmed Salem, Yang Zhang, Mathias Humbert, Pascal Berrang, Mario Fritz, and Michael Backes. MI-leaks: Model and data independent membership inference attacks and defenses on machine learning models. *arXiv preprint arXiv:1806.01246*, 2018.
- Reza Shokri and Vitaly Shmatikov. Privacy-preserving deep learning. In *Proceedings of the 22nd ACM SIGSAC conference on computer and communications security*, pages 1310–1321, 2015.
- Reza Shokri, Marco Stronati, Congzheng Song, and Vitaly Shmatikov. Membership inference attacks against machine learning models. In *2017 IEEE Symposium on Security and Privacy (SP)*, pages 3–18. IEEE, 2017.
- Florian Tramèr, Fan Zhang, Ari Juels, Michael K Reiter, and Thomas Ristenpart. Stealing machine learning models via prediction apis. In *25th {USENIX} Security Symposium ({USENIX} Security 16)*, pages 601–618, 2016.
- Zhibo Wang, Mengkai Song, Zhifei Zhang, Yang Song, Qian Wang, and Hairong Qi. Beyond inferring class representatives: User-level privacy leakage from federated learning. In *IEEE INFOCOM 2019-IEEE Conference on Computer Communications*, pages 2512–2520. IEEE, 2019.
- LeCun Yann, Cortes Corinna, and J.C. Burges Christopher. The mnist database of handwritten digits. <http://yann.lecun.com/exdb/mnist/>, 1998. Online; accessed 29-June-2021.
- Jason Yosinski, Jeff Clune, Yoshua Bengio, and Hod Lipson. How transferable are features in deep neural networks? In *Proceedings of the 27th International Conference on Neural Information Processing Systems - Volume 2, NIPS'14*, page 3320–3328, Cambridge, MA, USA, 2014. MIT Press.
- Hongyi Zhang, Moustapha Cisse, Yann N Dauphin, and David Lopez-Paz. mixup: Beyond empirical risk minimization. *arXiv preprint arXiv:1710.09412*, 2017.
- Bo Zhao, Konda Reddy Mopuri, and Hakan Bilen. idlg: Improved deep leakage from gradients. *arXiv preprint arXiv:2001.02610*, 2020.
- Ligeng Zhu and Song Han. Deep leakage from gradients. In *Federated Learning*, pages 17–31. Springer, 2020.